The Groundwater Flow Behavior and the Recharge in the Nubian Sandstone Aquifer System during the Wet and Arid Periods

Mohamed, Ahmed; Ahmed, Ezzat; Alshehri, Fahad; Abdelrady, Ahmed

DOI
10.3390/su14116823

Publication date
2022

Document Version
Final published version

Published in
Sustainability (Switzerland)

sustainability

MDPI

Article

The Groundwater Flow Behavior and the Recharge in the Nubian Sandstone Aquifer System during the Wet and Arid Periods

Ahmed Mohamed [1,*], Ezzat Ahmed [1], Fahad Alshehri [2,*] and Ahmed Abdelrady [3]

[1] Geology Department, Faculty of Science, Assiut University, Assiut 71516, Egypt; ezzat_abdallah@aun.edu.eg
[2] Abdullah Alrushaid Chair for Earth Science Remote Sensing Research, Geology and Geophysics Department, College of Science, King Saud University, P.O. Box 2455, Riyadh 11451, Saudi Arabia
[3] Department of Water Management, Faculty of Civil Engineering and Geoscience, Delft University of Technology, Stevinweg 1, 2628 CN Delft, The Netherlands; a.r.a.mahmoud@tudelft.nl
* Correspondence: ahmedmohamed@aun.edu.eg (A.M.); falshehria@ksu.edu.sa (F.A.); Tel.: +20-1008390135 (A.M.); +966-0114677053 (F.A.)

Abstract: The Nubian Sandstone Aquifer System (NSAS) is made up of three major sub-basins: Kufra, Dakhla, and the N. Sudan Platform. It is one of the world's largest groundwater systems. The aquifer's hydrologic setting, connectivity of its sub-basins, and groundwater flow across these sub-basins are currently unclear. To address these issues, we used a combined approach that included: (1) a regionally calibrated groundwater flow model that mimics early (>10,000 years) steady-state conditions under wet climatic periods and later (<10,000 years BP–1960; 1960–2010) transient conditions under arid climatic periods; and (2) groundwater ages (^{36}Cl, ^{81}Kr) and isotopic (^{18}O, ^{2}H) data. The NSAS was recharged on a regional scale in previous wet climatic periods; however, in dry periods, its outcrops are still receiving local modest recharge. A progressive increase in ^{36}Cl groundwater ages was found along groundwater flow directions and along structures that are sub-parallel to the flow direction. The NE–SW Pelusium mega shear zone is a preferential groundwater flow conduit from the Kufra to the Dakhla sub-basin. The south-to-north groundwater flow is hampered by the Uweinat–Aswan basement uplift. The findings provide useful information about the best ways to use the NSAS.

Keywords: NSAS; groundwater flow model; ages data

Citation: Mohamed, A.; Ahmed, E.; Alshehri, F.; Abdelrady, A. The Groundwater Flow Behavior and the Recharge in the Nubian Sandstone Aquifer System during the Wet and Arid Periods. *Sustainability* **2022**, *14*, 6823. https://doi.org/10.3390/su14116823

Academic Editors: Ashwani Kumar Tiwari, Subhash Chandra and Carlos Silva

Received: 14 March 2022
Accepted: 24 May 2022
Published: 2 June 2022

1. Introduction

Despite the fact that NE Africa is one of the world's driest places, geological evidence reveals that during the Quaternary Episode, the climate cycled between arid and wet periods, with the most recent major rainy period occurring in the Holocene (10,000 years ago). The groundwater in the Nubian Sandstone Aquifer System (NSAS, Figure 1) was replenished thousands to millions of years ago by intensification of paleo-monsoons [1–3] or paleo-westerlies [4,5]. All the previous models argue that recharge was performed predominantly by precipitation over more distant mountains (Ennedi, Erdi, Tibesti) (e.g., [6,7].

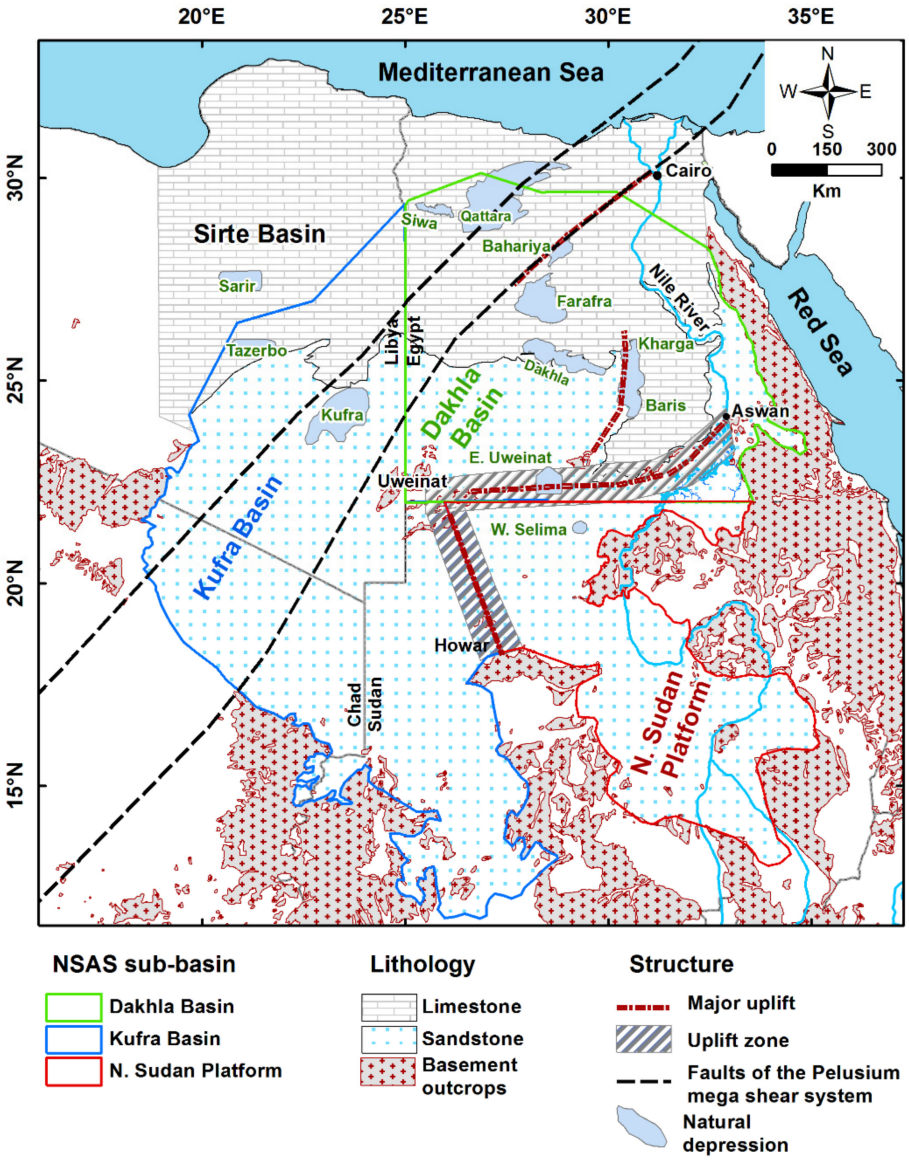

Figure 1. Location map showing the distribution of the NSAS, sub-basins, basement uplifts, and faults of the PMS system within the aquifer.

Refs. [6,7] were the first to characterize regional flow, observing a regular gradient in the groundwater levels at observation wells in Egypt, Libya, Chad, and Sudan. They made a net of contour lines (Figure 2) and discovered that groundwater flow follows a gradient from some unknown "intake beds" in the southwest to the Egyptian oasis. This concept has been retained in all prior regional models to date. These models, on the other hand, do not mimic flow from locations where recent recharging may have occurred, nor do they predict groundwater recharge in areas that have been treated in our current model. Ref. [8] described how the aquifer was refilled by recharge from the southwest. In the Ennedi, Uweinat, and Gilf Kebir highlands, they found that a steady state could be maintained with only a 10 mm/y recharge.

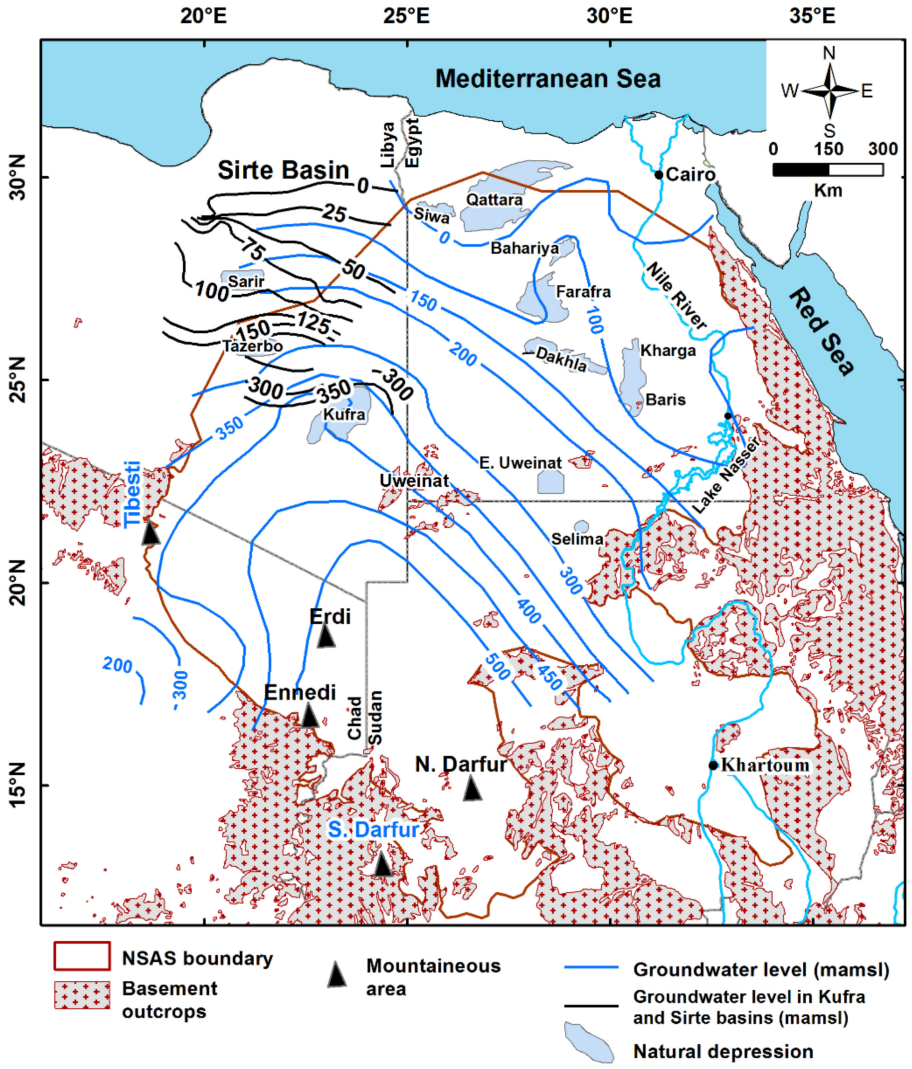

Figure 2. Groundwater contour lines after [6,7]. Also shown are the piezometric contour lines in Kufra and Sirte basins after [9].

NSAS is crucial since it is the only viable source of water for future development plans in NE Africa's arid regions. Egypt and Libya, faced with overpopulation issues and a need to create additional agricultural fields to sustain their growing populations, established plans to develop and utilize the aquifer over the previous three decades. As a result, the NSAS is heavily exploited in these countries for agricultural and drinking water purposes. The Libyan government has announced that the Great Man-made River project (GMMR) will begin collecting significant volumes of water from this aquifer.

Rising temperatures, changes in precipitation patterns, inland evaporation, and salinization are all projected to exacerbate the effects of climate change. The average annual precipitation over the recharge areas in the S. Kufra and N. Sudan Platform sub-basins has been estimated at 54.8 and 32.8 km^3, respectively, based on Tropical Rainfall Measuring Mission (TRMM) data; Gravity Recovery and Climate Experiment (GRACE) and outputs of the climatic (CLM4.5) model [10] support the presence of substantial recharge rates of 0.78 $\pm$ 0.49 and 1.44 $\pm$ 0.42 km^3/y over S. Kufra and N. Sudan Platform sub-basins, respectively. The radiocarbon and stable isotope results also indicate the presence of local recharging by contemporary water [11–13]. Through studying their isotopic signatures, the Nubian Sandstone aquifer in Wadi El-Trafa and the Sinai Peninsula is receiving contemporary water under the current dry climatic circumstances [14,15].

GRACE has frequently been utilized to estimate aquifer recharge and depletion rates, as well as mass variations across vast areas, in conjunction with other relevant meteorological information (e.g., [10,16–37]).

The current study aimed to answer some questions that had previously been unanswered by previous regional groundwater flow models: how large the early Holocene paleo-recharge rate was; where the groundwater was recharged; how the groundwater flowed during the filling-up process; and how the aquifer responds to climatic change, particularly during the transition from a wet to arid climate period and decreased infiltration. Our model accounts for the barrier along the Dakhla basin's southern border as well as the preferred groundwater flow pattern from the Kufra basin into the Dakhla basin. As a result, we focused our models on the increased hydraulic conductivities of the high permeability conductive sandstones that fill the northeast Pelusium conduit zone.

2. Geology

The NSAS is made up of continental Cambro-Ordovician to Upper Cretaceous sediments with some Devonian, Carboniferous, and Turonian marine intercalations [38–41]. The Nubian Sandstone layers are overlain by a massive accumulation of Upper Cretaceous-Tertiary sea sediments to the north of the study area. According to [12], the aquifer is unconfined south of latitude 25° and confined north of it. The thick (several hundred meters) marine shales and clays of the Campanian Mut Formation and the Campanian to Lower Paleocene Dakhla Formation are the restricting layers [12]. The NSAS is divided into three sub-basins (Figure 1). The Dakhla sub-basin in Egypt and northern Sudan platform, as well as the Kufra sub-basin in Libya, northeastern Chad, and northwestern Sudan. The thickness of the NSAS varies spatially along these sub-basins (maximum thickness: Kufra: ~2.5–4 km; Dakhla ~1–3 km; northern Sudan platform: ~0.5 km [12,42].

Despite the fact that the northern Sudan platform is separated from the Dakhla sub-basin by an east–west trending basement uplift (Uweinat–Aswan uplift), the northern Sudan platform is partially separated from the Kufra suction basin by another SE–NW trending uplift (Uweinat–Howar uplift), and the Kufra and Dakhla sub-basins are connected by NE–SW trending shear zone structures; the vast majority, if not all, existing regional groundwater flow models for the NSAS treat it as a continuous basin (e.g., [43–45]).

3. Climate

The Earth's climate has oscillated many times over the last 2.6 million years (the Quaternary Period), swinging between glacial and interglacial regimes. Large ice ages and interglacials with a periodicity of roughly 100,000 years have occurred throughout the last 1 million years. Large ice sheets formed in mid- to high-latitudes throughout the glacial period, notably across Britain and North America. Changes in the Earth's orbit around the sun are responsible for these enormous shifts. We are currently experiencing an interglacial period [46].

Although the northwestern part of Sudan and the southwestern part of Egypt are currently among the driest parts of the Sahara [47], archaeological sites associated with remnants of playa or lake deposits reveal past periods of high effective moisture. Geoarchaeological investigations at Neolithic playa sites in Egypt [48–50] and ancient lake bed sites in northern Sudan [51–55] have generally documented an early Holocene pluvial cycle.

4. Material and Methods

The model was created to examine the aquifer's regional behavior. Thus, a groundwater flow model was built by identifying model boundaries and initial conditions, then calibrating it over early steady-state conditions under wet climatic conditions (>10,000 years ago), and later long (10,000 years ago–1960) and short (1960–2010) transient conditions under arid climatic conditions. The model for the NSAS in the research area was developed using Groundwater Modelling Simulation (GMS, 10.2).

4.1. Model Domain

The NSAS domain stretches about ~2.2 × 10^6 km^2 and crosses the political borders of Egypt, Sudan, Chad, and Libya (Figure 1). The position of the NSAS southern limit in Sudan and Chad was chosen to incorporate all sediments and end when basement rocks outcrop. This extended the southern boundary of the previous major body of the NSAS, which had been established by a number of researchers [8,45,56]. The eastern boundary was chosen based on earlier research findings at a site near the Red Sea crystalline rocks, where the Nubian sands vanish.

The western limit of the Tibesti Mountain was chosen as the area where NSAS sediments disappear and basement appears. Jebel Uweinat was chosen as an internal border where NSAS permeable sediments vanish and older igneous and volcanic rocks of higher relief occur in the same place. Due to a paucity of data to the north, the fresh saline water interface was chosen as the northern boundary rather than the Mediterranean coast. The ground surface level was used to determine the top of the NSAS aquifer, which was received from the Shuttle Radar Topography Mission (SRTM 3 arc-second data, Figure 3a). The sediment thickness of the NSAS was calculated as the difference between the ground surface and basement level, with the bottom boundary fixed at the underground crystalline basement rocks and was treated as one layer with a grid size of 20,000 m. Figure 3b shows that the NSAS thickness increases northwards from 500 m in the northern Sudan Platform and along the southern parts of the Dakhla Basin in places near the Uweinat-Aswan uplift to more than 4 km near the aquifer's northern boundary [10].

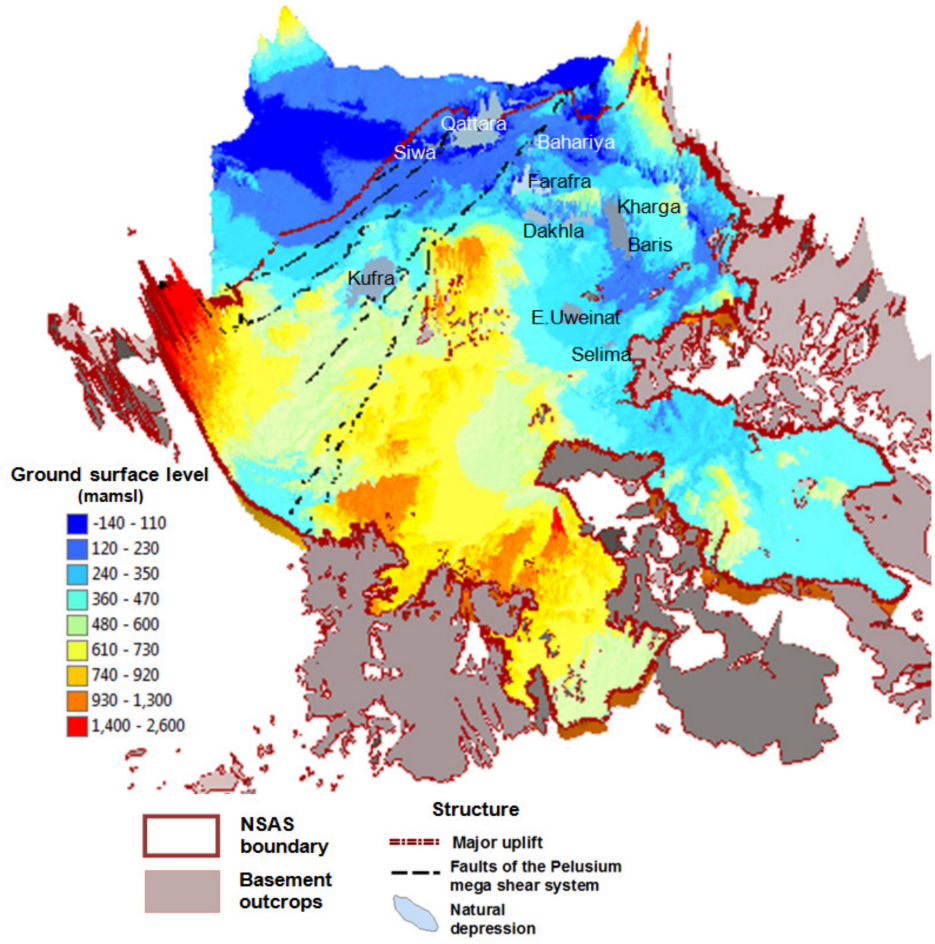

(**a**)

Figure 3. *Cont.*

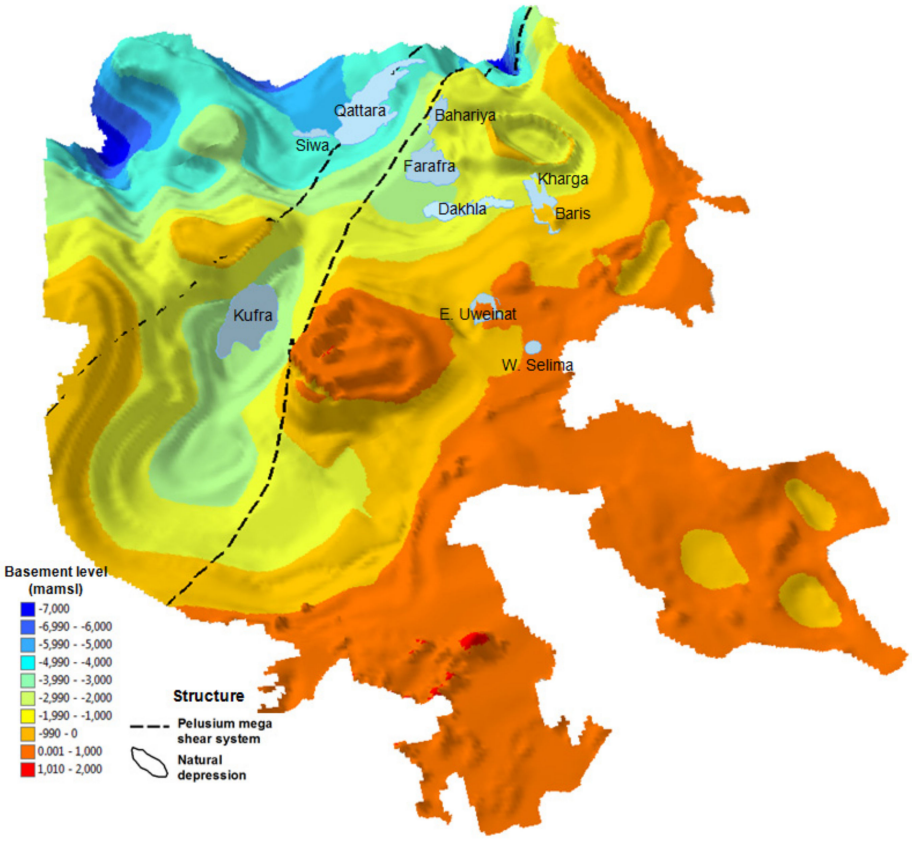

(**b**)

Figure 3. Basin geometry: (**a**) Ground surface level of the aquifer derived from SRTM; and (**b**) basement relief 3D image generated over NSAS showing thickening of the sedimentary sequences to the north, and along the northeast-trending Pelusium mega shear zone.

4.2. Initial and Boundary Conditions

The model was created with the goal of accurately simulating the NSAS water level in the last wet (>10,000) and dry (<10,000) periods. In addition to the most recent anthropogenic effects, climatic change plays an important role in the water decline over time, as groundwater decline has been occurring naturally in response to climatic change since the last pluvial period and will continue until the next pluvial period in the future. The aquifer was believed to be saturated during the pluvial period [8] to imitate the NSAS and was largely recharged prior to and/or during the Last Glacial Maximum [57].

The presence of surface (Figure 4) and near-surface paleo-drainages in the Kufra area (Figure 5a) flowing northwards from north Chad and Sudan across the Libyan Desert strongly suggests that the aquifer was filled to the surface from sandstone outcrops in the southern half. The filling-up of the aquifer is also indicated by the watersheds in the southern section of the Dakhla Basin (Figure 5b) in the Uweinat area. Furthermore, playa deposits (Figure 5c) were discovered along scarps in the Western Desert, which were identified as Kharga depression deposits.

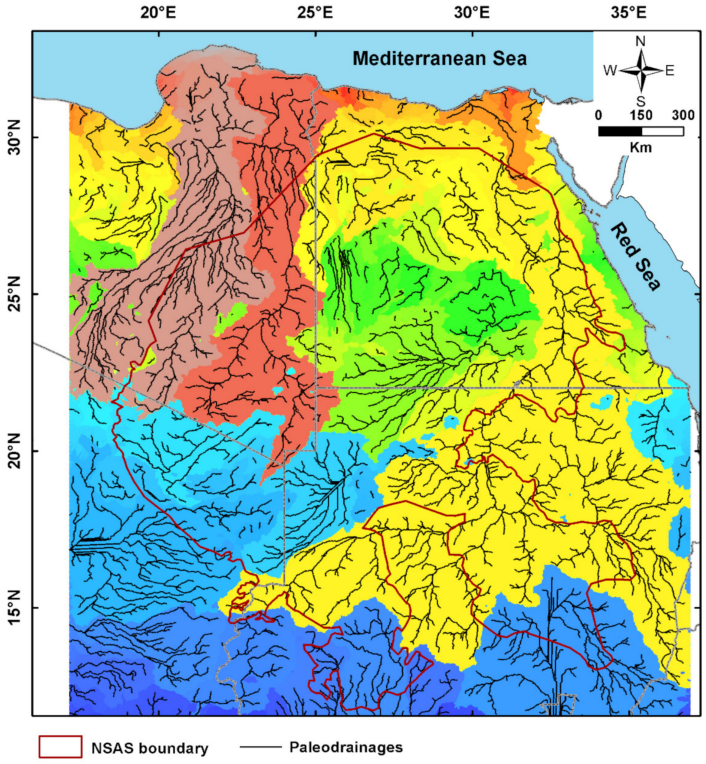

Figure 4. Paleo-drainages over NE Africa derived from SRTM 3 arc-second.

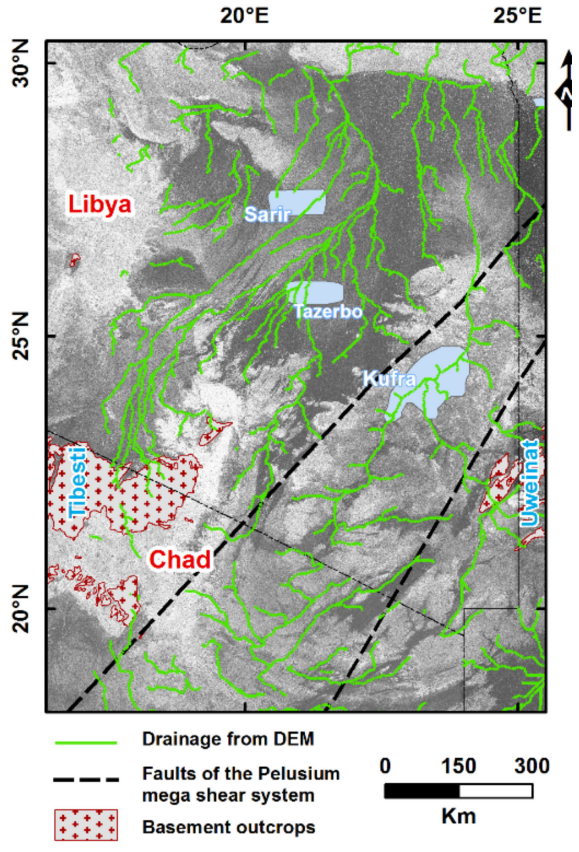

(**a**)

Figure 5. *Cont.*

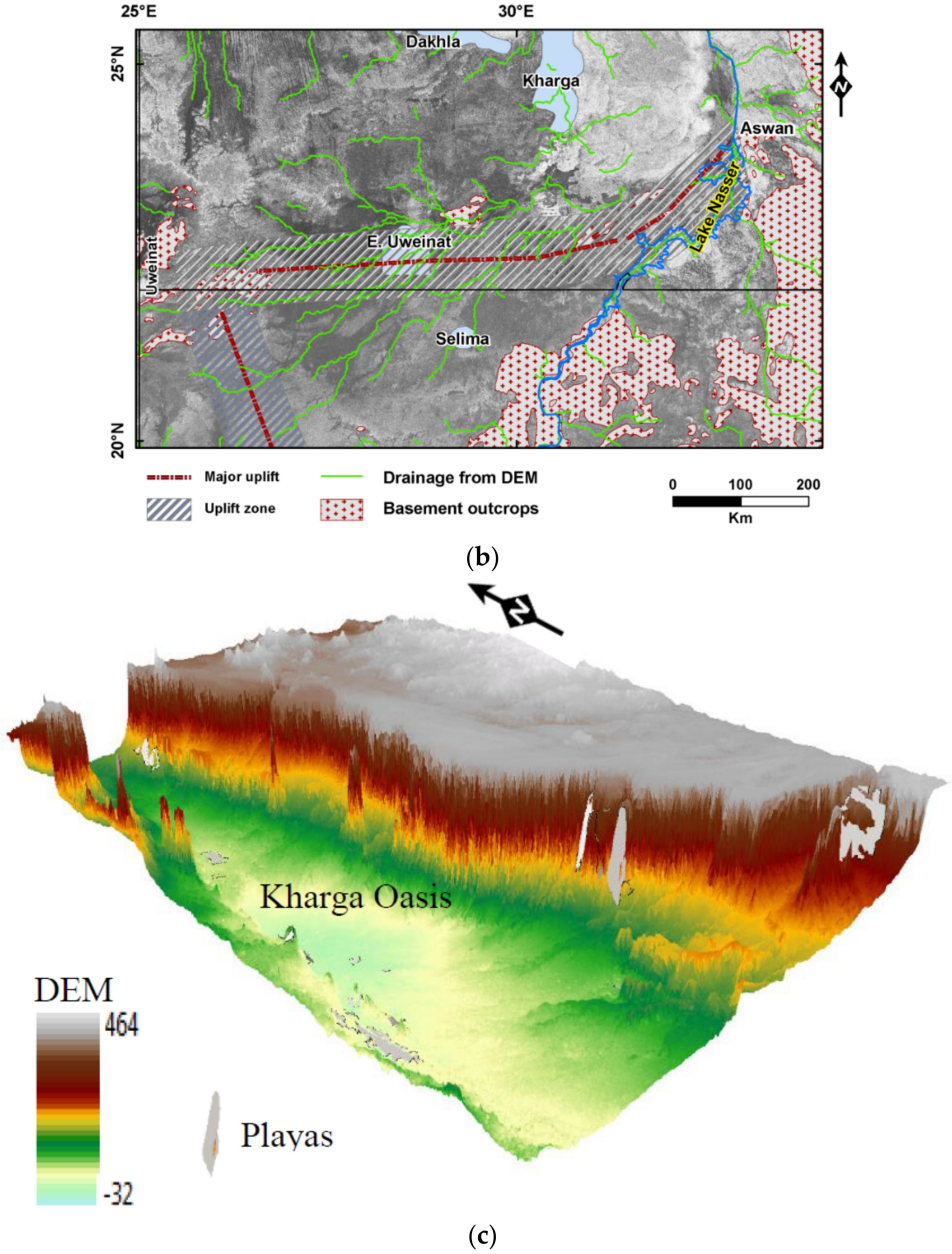

Figure 5. (**a**) Kufra and (**b**) Uweinat paleo-drainages mapped using SRTM and RadarSat images; and (**c**) playa deposits along the scarp of the Kharga depression.

No-flow regions are depicted on the eastern, southern, western, and bottom edges, where no groundwater can flow; the internal boundary of Jebel Uweinat is also depicted as no-flow. During the transient simulation, the saline–fresh water interface was defined as the northern and northwestern boundary, which was altered from no-flow during the steady state to a time-variant specified head. The top border was utilized to pass recharge water to specific locations and remove water from discharge zones. The southern sandstone outcrops were given recharge zones, whereas the northern discharge areas were given drain conditions.

4.3. Model Calibration

Before using the model to forecast the system's reaction to any developmental activity, it should be calibrated. Model calibration is the process of fine-tuning a model's input parameters (hydraulic conductivity, specific storage, porosity, recharge, and drain rate)

and boundary conditions to achieve a close match to observed data (e.g., hydraulic head, flow rate) in a real-world groundwater system. The hydraulic conductivities, which were intergraded across the entire sediment thickness (taken from [56]; Figure 6) and changed based on the available pumping tests, are the most essential parameter ([58], Table 1). It was changed little to calibrate the model in the steady state filled-up stage. In a flow model calibration, simulated heads, and Darcy fluxes are frequently compared to their observed counterparts. If a model is properly calibrated, there will be some random discrepancies between simulated and observed data, but no systematic variances. If there are systematic inaccuracies, such as when the majority of the simulated heads exceed the actual heads, the calibration is insufficient. It is necessary to make adjustments.

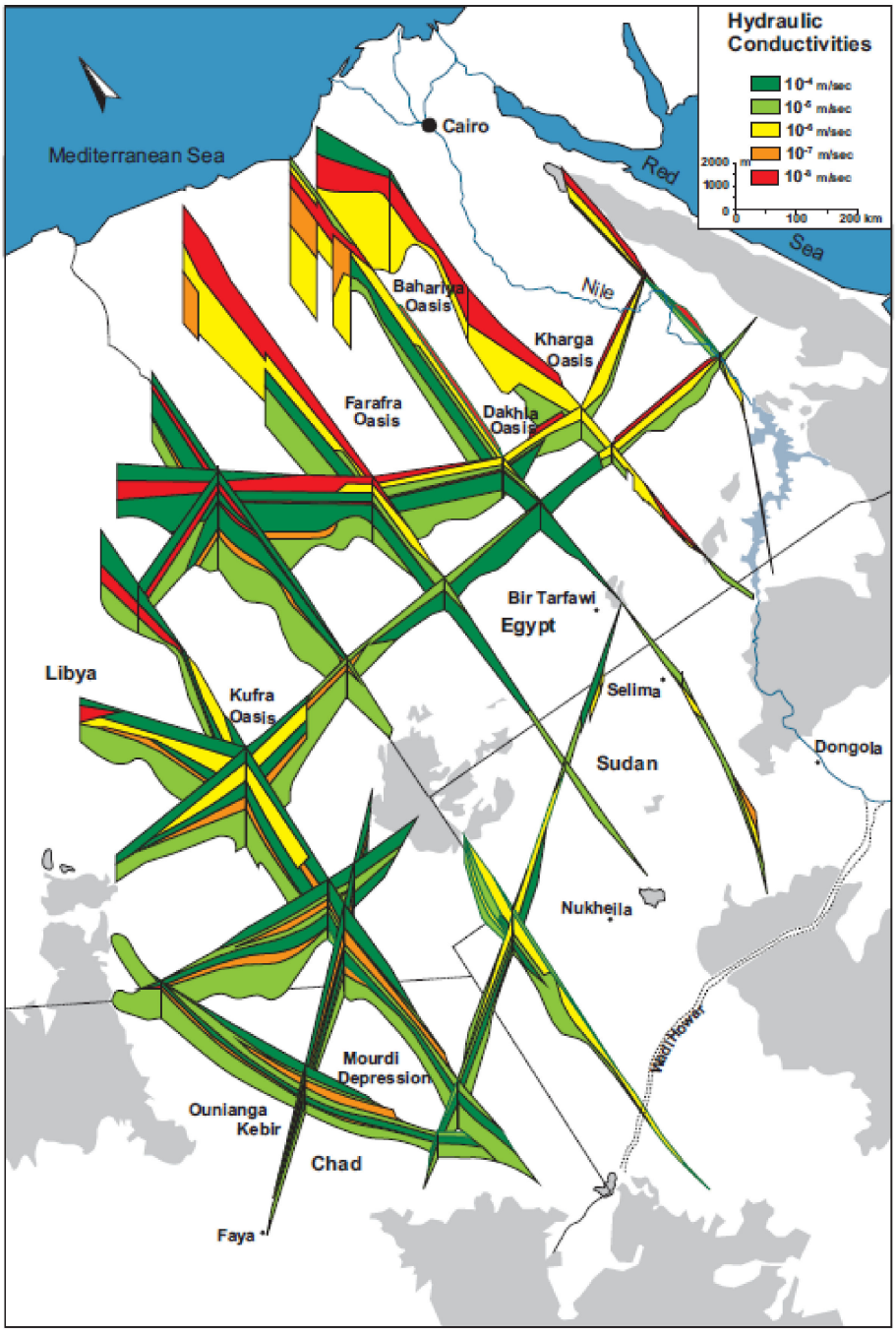

Figure 6. Zonation of hydraulic conductivity in the aquifer (after [56]).

Table 1. Average hydraulic conductivity parameters of the Nubian Aquifer System.

Region	Country	Number of Pumping Tests	Hydraulic Cond. (m/s)	Storage Coefficient	Region	Country	Number of Pumping Tests	Hydraulic Cond. (m/s)	Storage Coefficient
Wadi Qena	Egypt	6	3.960×10^{-6}		Aswan	Egypt	1	2.778×10^{-5}	
Wadi ElLaquita	Egypt	2	1.980×10^{-5}		Tazerbo	Libya	5	9.400×10^{-5}	
Bahariya	Egypt	10	4.300×10^{-5}	8.00×10^{-4}	Kufra	Libya	60	5.030×10^{-5}	2.34×10^{-3}
Farafra	Egypt	8	5.400×10^{-5}		West Selima	Sudan		1.436×10^{-4}	1.43×10^{-4}
Abu Munqar	Egypt	3	2.180×10^{-4}		El Atrun	Sudan		1.500×10^{-4}	
Dakhla	Egypt	21	6.100×10^{-5}	6.35×10^{-4}	West Howar	Sudan		4.400×10^{-5}	
Kharga	Egypt	59	2.900×10^{-5}	2.84×10^{-4}	Um Hilal	Sudan		3.300×10^{-4}	
East Uweinat	Egypt	6	1.300×10^{-4}		El Hashi	Sudan		2.390×10^{-4}	
Siwa	Egypt		3.420×10^{-4}		Dongola	Sudan	29	1.180×10^{-3}	

Source: [58].

4.3.1. Steady State Filled-Up Stage

The calibration in this stage was carried out to achieve a close fit between the simulated heads and the ground surface levels. In the last pluvial period, the aquifer was assumed to be filled up to the surface through the water-bearing sandstones in the southern part. Inspection of Figure 7a,b shows that the simulated head contour lines are similar to those smoothed contour lines on the ground surface. A total of well distributed 500 elevation points were assigned in the model in the calibration technique. Computed heads versus observed ground surface points (Figure 7c) show a good correspondence of 0.95. During that period, the infiltration rates (Figure 8) were estimated at 2–7 mm/y in plains and 10–27 mm/y at highlands with a total average of ~8.13 mm/y (13.07 km^3/y). A similar recharge rate of 10 mm/y was reported by [8]. Inspection of Figure 8 shows the NSAS was recharged at the foothills of the mountainous areas of Ennedi, Erdi, Tibesti, Uweinat, and Red Sea where the rainfall rates were higher than those of the plains.

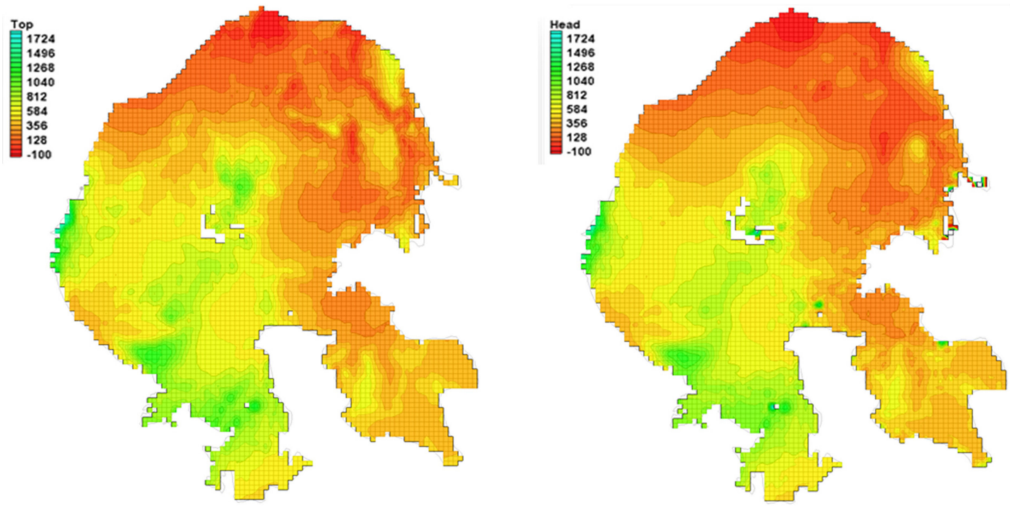

(**a**) (**b**)

Figure 7. *Cont.*

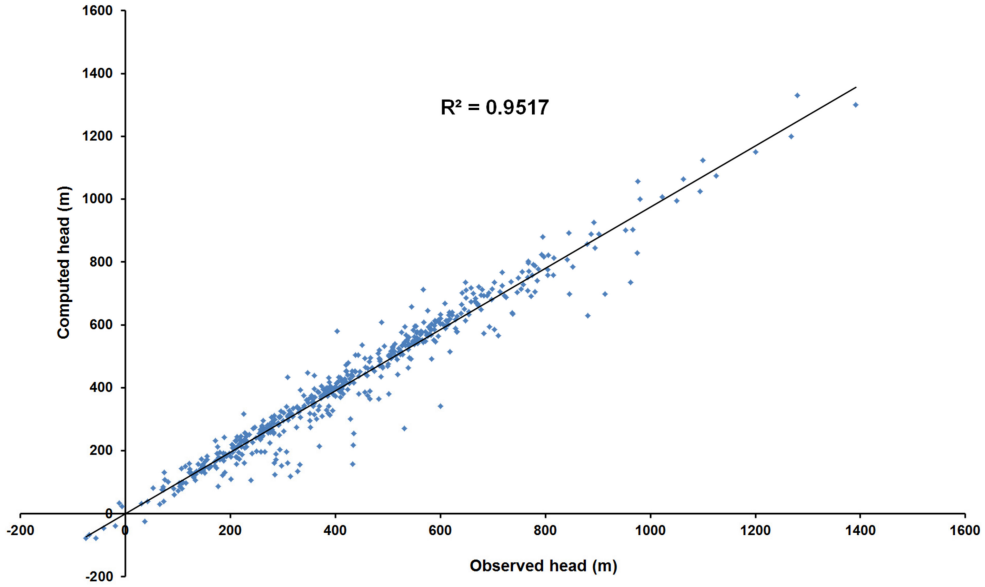

(**c**)

Figure 7. (**a**) Surface elevation of the aquifer; (**b**) simulated groundwater contour lines for a steady state; and (**c**) observed versus computed head at observation points.

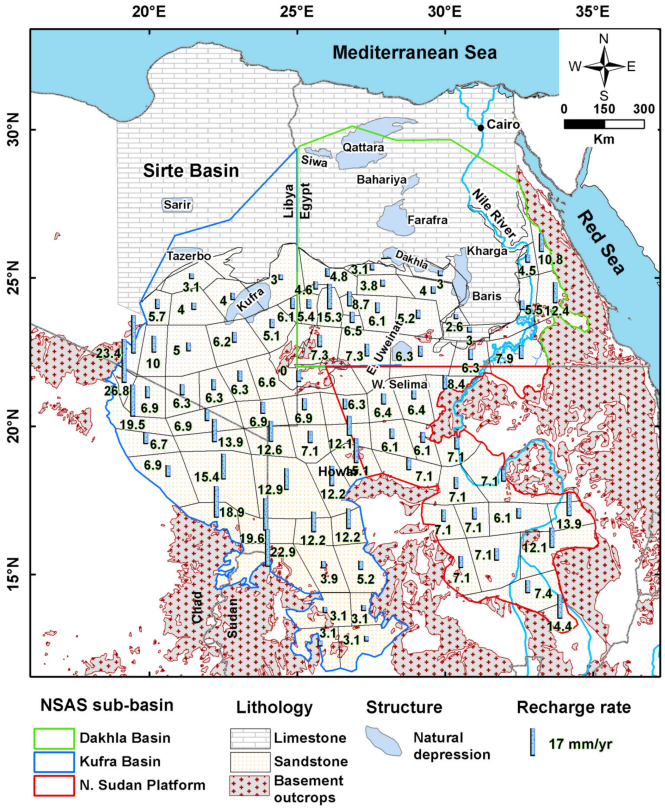

Figure 8. Pelo-recharge estimated for the steady state filled-up condition in the last pluvial period (>10,000 y BP).

This little recharge rate applied to the sandstone outcrops was enough to keep the aquifer full to some extent and more closely to the ground surface. However, a complete fill-up in all the areas may not be possible, as the groundwater heads in the highlands will be far below the ground surface or will rise above the ground surface on extended areas in the plains and cause large drain areas.

4.3.2. Long-Term Transient Stage

The transient simulation was carried out to simulate the behavior of the aquifer in response to climatic change in the dry period after decreasing the infiltration rate by the end of the last wet period (~10,000 y Before Present). The calibration in this stage was conducted against the groundwater contour lines, measured by [6,7], which represents the groundwater level in the aquifer before beginning of the heavy exploitation in 1960. We changed the applied recharge rates of the steady-state stage across the aquifer to get a good fit between the modeled heads and the groundwater lines of [6]. The groundwater velocity was estimated from the distribution of the ages, given that these ages might give better values. Hence, the hydraulic conductivity values were calibrated against the groundwater velocity derived from the ages. For this stage, 50 time steps were applied.

The simulated groundwater contour lines (Figure 9a) of this stage show a similar shape as Ball's contour lines with a good correspondence (Figure 9b) between the observed heads and the computed hydraulic heads. The long transient simulation results indicate that the continuous decline in the water level of the aquifer was naturally along the depressions, paleo-drainages, and Nile River. This is called a natural discharge which may continue to current day. That water decline in the aquifer almost started about 10,000 years ago, but it was slowed down by local infiltrations occurring in the highlands and other parts of the system. Young C-14 groundwater ages were reported from south of the Uweinat-Aswan uplift in the east Uweinat area (1.8–11.3 $\times$ 10^3 y; [11]) indicating modern recharge within the dry period.

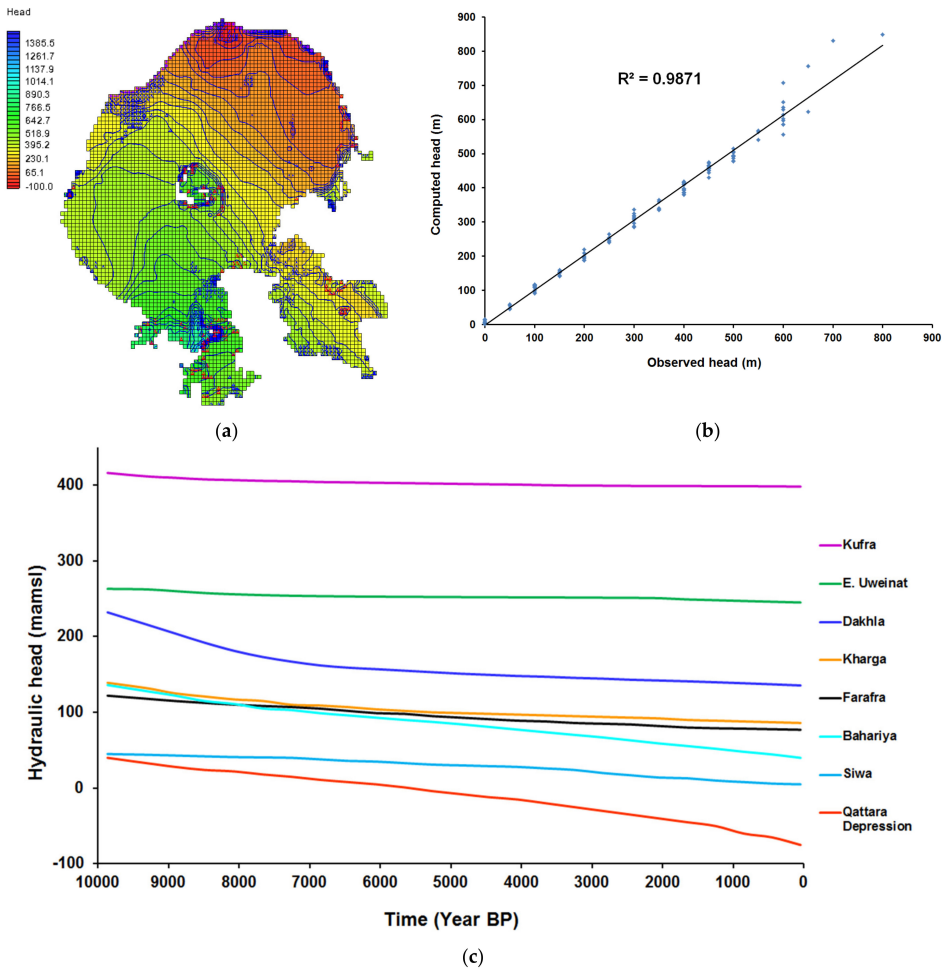

Figure 9. (**a**) Simulated groundwater head for the NSAS befroe the development (1960); (**b**) computed versus observed head [6]; and average discharge time series of groundwater head at oases and depressions; and (**c**) hydrographs of drawdown for various discharge oases.

Inspection of Figure 9c shows the average drawdown of the water level in the depression and oases through the dry climate over the past 10,000 years in the northern part of the aquifer. In such conditions, the rate of infiltration from the highlands is insufficient to maintain other shallow oases (Nukheila, Atrun, Laquia Arbain) in the southern elevated areas. After 4–5 $\times$ 10^3 y from the late pluvial period, Kufra Oasis has become dry. However, these shallow oases are promising areas for agricultural development in their regions.

During the dry period, the groundwater level dropped rapidly in the elevated recharge areas after decreasing the infiltration rate; it dropped about 70 m in 1000 y in Ennedi and Gilf Kebir. Moreover, it dropped more than 100 m in the Tibesti area and Red Sea hills. In the depressions, no considerable draw-down below ground surface as they remain natural discharge area. Our results were in a good agreement with those of [8].

During that period, the annual recharge rate was estimated at 0.42–1.14 mm/y in plains and at 1.16–5.36 mm/y at the foothills of the mountainous areas (Figure 10). The total average annual recharge rate was calculated at 1.3 mm/y (1.6 km^3/y).

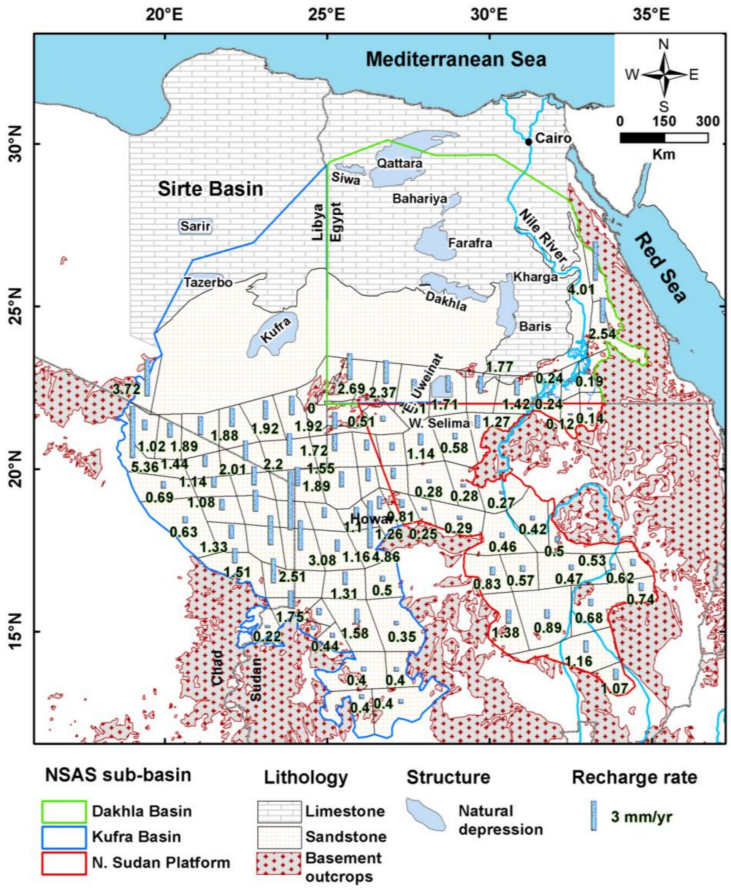

Figure 10. Paleo-recharge estimated from the long transient condition for the arid period (<10,000 y BP).

4.3.3. Short-Term Transient Stage (1960–2010)

The aim of this calibration is to check the assumptions made in the long-term transient simulation and to better understand the aquifer behavior to the gradual increase of the extraction rates between 1960 and 2010 across 50 time steps. Therefore, the hydrologic parameters from the transient long-term flow stage have been taken, and modified during the transient short-term simulation. Oases were given an evapotranspiration value of 10–15 mm/y. [59–61] instead of the drain boundary. The modification in the parameters was carried based on the available pumping tests and measured heads. Figure 11 shows the simulated groundwater level in 2010, which still maintain the groundwater countour lines of [6]. The linear regression analysis of computed heads versus observed heads for wells shows a good correlation (Figure 12a,b).

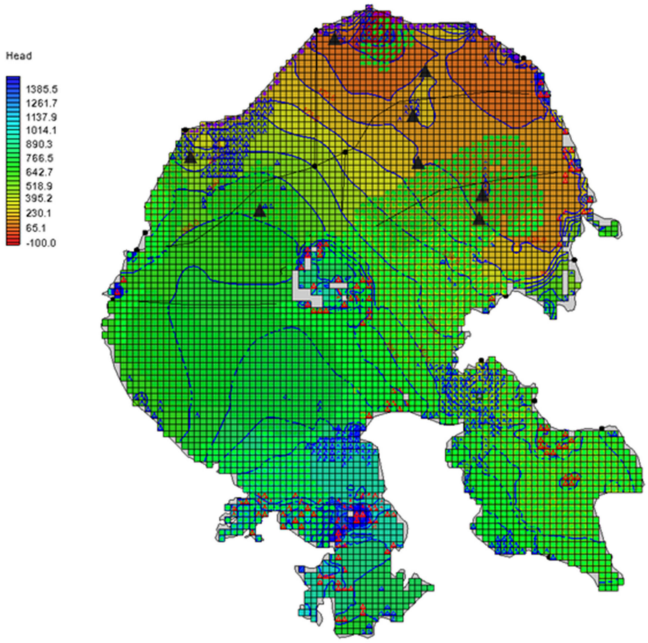

Figure 11. Simulated groundwater level 2010 in the NSAS.

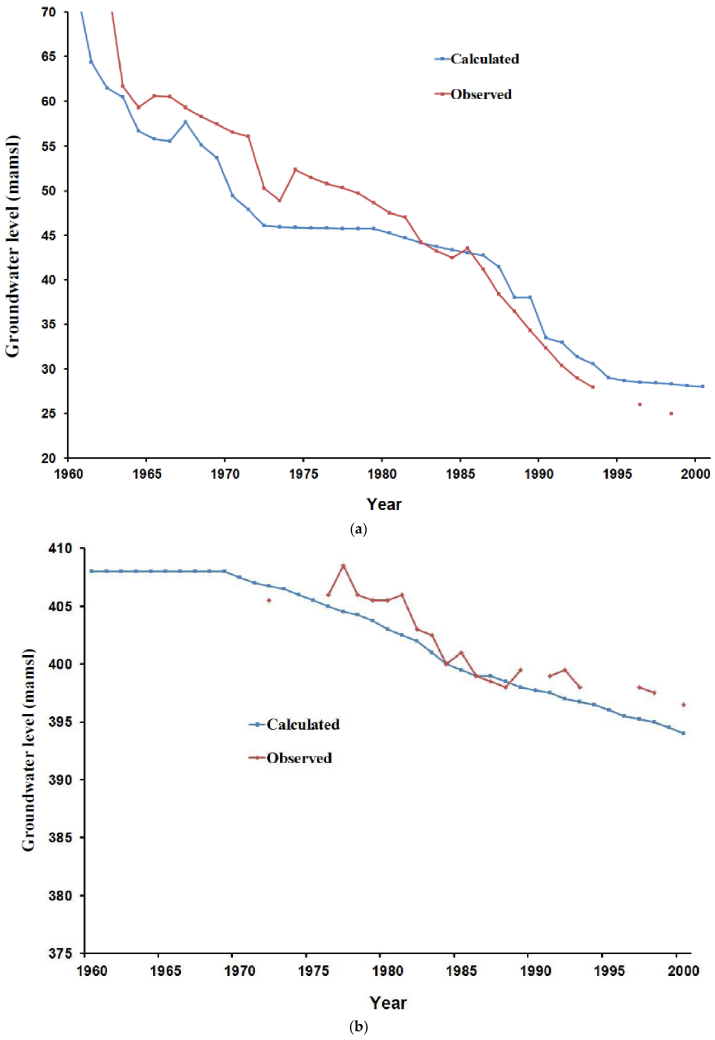

Figure 12. Variation of groundwater level for (**a**) a well in Kharga and (**b**) a well in Kufra.

With a gradual increase in extraction rates in the developing areas from 1960 to 2010, the groundwater level is gradually declining in those areas leading to a gradual drecrease in the natural discahrge with time which has stopped in some oases. The annual discharge rate at Qattara depression may reach up to 0.76 km^3/y, while that due to the Nile River in Sudan may reach up to 0.062 km^3/y and vary from 0.050 to 0.040 km^3/y for the Nile river in Egypt. The annual recharge rate from Lake Nasser was estimated at 135 × 10^6 m^3/y which may help replenish the groundwater in Tushka area.

5. Evidence Supporting the Groundwater Flow Paths

Groundwater has flowed in a NW direction from Erdi highlands following the basement relief and then redirected to the NE direction along the major structural lows that formed along the NE–SW Pelusium shear zone (Figure 13) from NW Chad and SE Libya into Egypt, especially at the lower levels. As shown by relatively high hydraulic conductivities, this zone could provide a preferential groundwater flow conduit from the Kufra to the Dakhla Basin (Kufra area: 5 × 10^{-5} m/s; north Daklha area: 5 × 10^{-5}–3.42 × 10^{-5} m/s; [58] and thickness of the Paleozoic–Lower Cretaceous sandstones (Kufra area: ~2.5–4 km; north Daklha area: ~2–3.5 km) [12,42] within this zone compared to its surroundings.

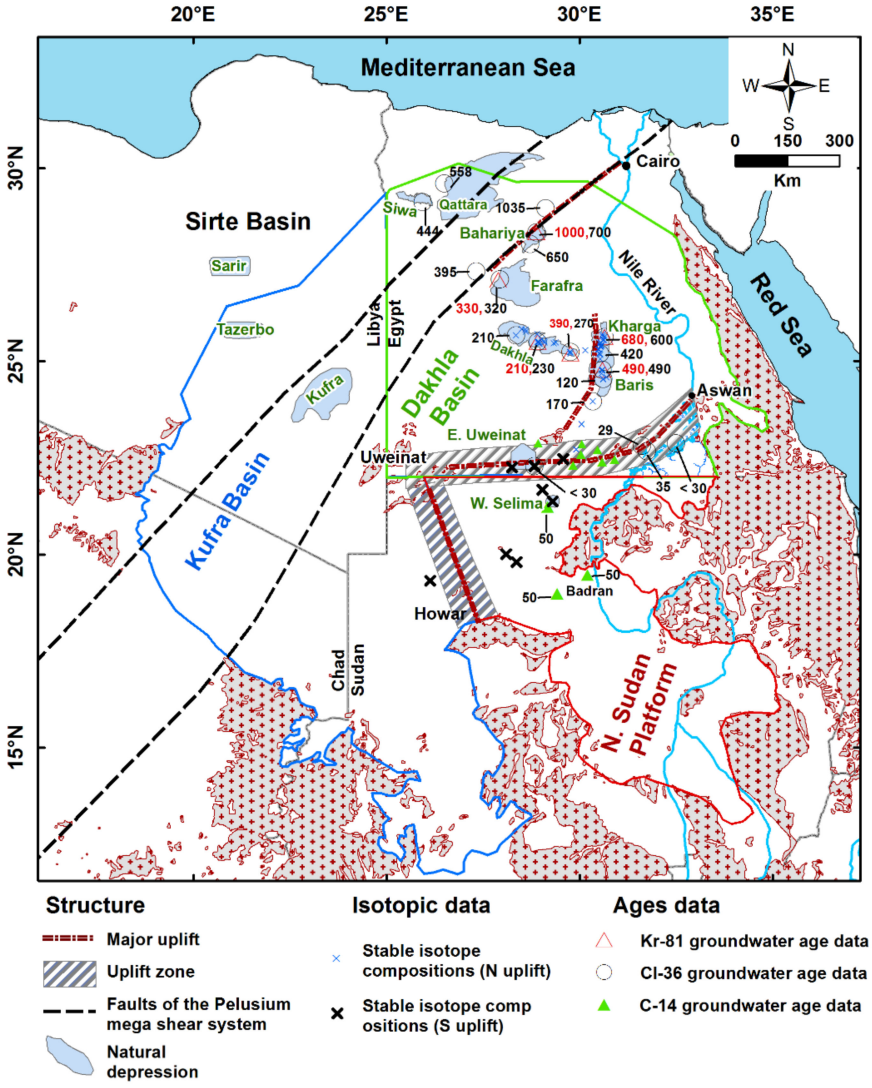

Figure 13. Locations of dated in 10^3 y (Kr-81: [5]; Cl-36: Current study; [62]; C-14: [11,63]) and isotopically (O, H) analyzed groundwater samples north and south of the Uweinat–Aswan uplift.

The progressive increase in ^{36}Cl groundwater ages (Figure 13) along the shear zone from Siwa (444 ky) to Qattara (558 ky) depression and from west Farafra (395 ky) to north Bahariya (1035 ky) strongly supports the flow sub-parallel to the shear zone. They also indicate relatively high flow velocities (Siwa to N. Baharyia: 1.68×10^{-8} m/s; W. Farafra to N. Baharyia: 1.27×10^{-8} m/s) along its zone in Egypt, which are consistent with our areal distribution of the hydraulic conductivity of the sandstones within the Nubian Aquifer with a different order of magnitude.

Furthermore, the groundwater ages increase progressively along the groundwater flow direction in the Dakhla Basin. Krypton-81 and chlorine-36 (Figure 13; [5,62]) show a progression of groundwater ages from Dakhla oasis (~210–230 ky) to Farafra oasis (~320–330 ky) with relatively high flow velocities (~1 m/y; 3.17×10^{-8} m/s) and with low flow velocities (~0.2 m/y; 6.34×10^{-9} m/s) from the Farafra to Bahariya (~1000 ky, Bauti-1). The presence of the NE–SW Cairo-Bahariya basement uplift (Figure 13) cutting in the northwestern part of the oasis along the southern border of the faults of the Pelusium shear zone impedes the groundwater flow from Farafra to Bahariya oasis reflecting low flow velocities.

However, eastwards from the Dakhla Oasis, the groundwater flow velocities have decreased due to the presence of the north–south trending basement Kharga–Bir Safsaf uplift, which obstructs west to east groundwater flow. Lithologically, this is supported by the presence of sediments of moderate permeability covered the Precambrian basement in the area between Bir Safsaf and Aswan. These sediments are composed of sandstones and siltstones equivalents of Sabaya and Maghrabi formations at the lower part. These deposits are covered by Kiseiba Formation with thickness of 100–250 m, which composed of alternating sandstones, siltstones, and shales with a northward increasing in the shale content from Bir Safsaf–Aswan uplift to the north [64]. Geochronologically, it is evidenced by the large differences in ages between groundwater samples on either side of the Kharga–Bir Safsaf uplift. The older ages of the samples west of the uplift are about 270–390 ky, which are relatively very younger in comparison to the very older ages (6000–680 ky) east of the uplift reflecting low hydraulic conductivity of ~0.2 m/y (6.34×10^{-9} m/s).

With the increase of water level declining in E. Uweinat area that resulted from the heavy anthropogenic effects after 1960, the northward groundwater flow from N. Sudan sub-basin has gradually redirected toward the east. Despite the N. Sudan Platform is still receiving modest recharge in the dry period indicated from the integration of GRACE and CLM4.5 model [10]; however, the effect of replenishment of the flow caused by that recharge does not appear in the northern part of the aquifer and excessive depletion is observed. This is partially hindered by the major east–west trending basement Uweinat–Aswan uplift. The differences in the isotopic compositions of groundwater on either side of the uplift (north-average $\delta^{18}O$: $-10.7‰ \pm 0.9‰$, average δD: $-80.8‰ \pm 3.9‰$; south-average $\delta^{18}O$: $-8.6‰ \pm 1.4‰$, average δD: $-40.8‰ \pm 5.6‰$; Figure 13) [65] support this suggestion. Bir Misaha trough with about one km wide and ~400–700 m deep in the western part of the Uweinat–Bir Safsaf uplift across the Sudanese-Egyptian border may act as a small conduit toward the north unless its shallowing southward in N. Sudan platform.

Not only does the Uweinat–Awan uplift (Figure 14a) obstruct the northward ground flow, but also the shallower basement in the northernmost part of the N. Sudan Platform affects the groundwater flow to the north. Based on the sedimentary cover in north of Sudan, a cross sectional area has been estimated to be ~90 km^2 along the line of groundwater level of 300 m between Gebel Uweinat and north Sudan basement rocks. Moreover, on the basis of a coefficient of hydraulic conductivity of $K = 1.3 \times 10^{-4}$ m/s and a hydraulic gradient of $h = 2.7 \times 10^{-4}$, the potential groundwater influx amounts to 99.5×10^6 m^3/y. Assuming no obstacles to groundwater flow, this low amount could not compensate for the current heavy extraction rates 47.56 m^3/s (1.5 km^3/y) in the East Uweinat area.

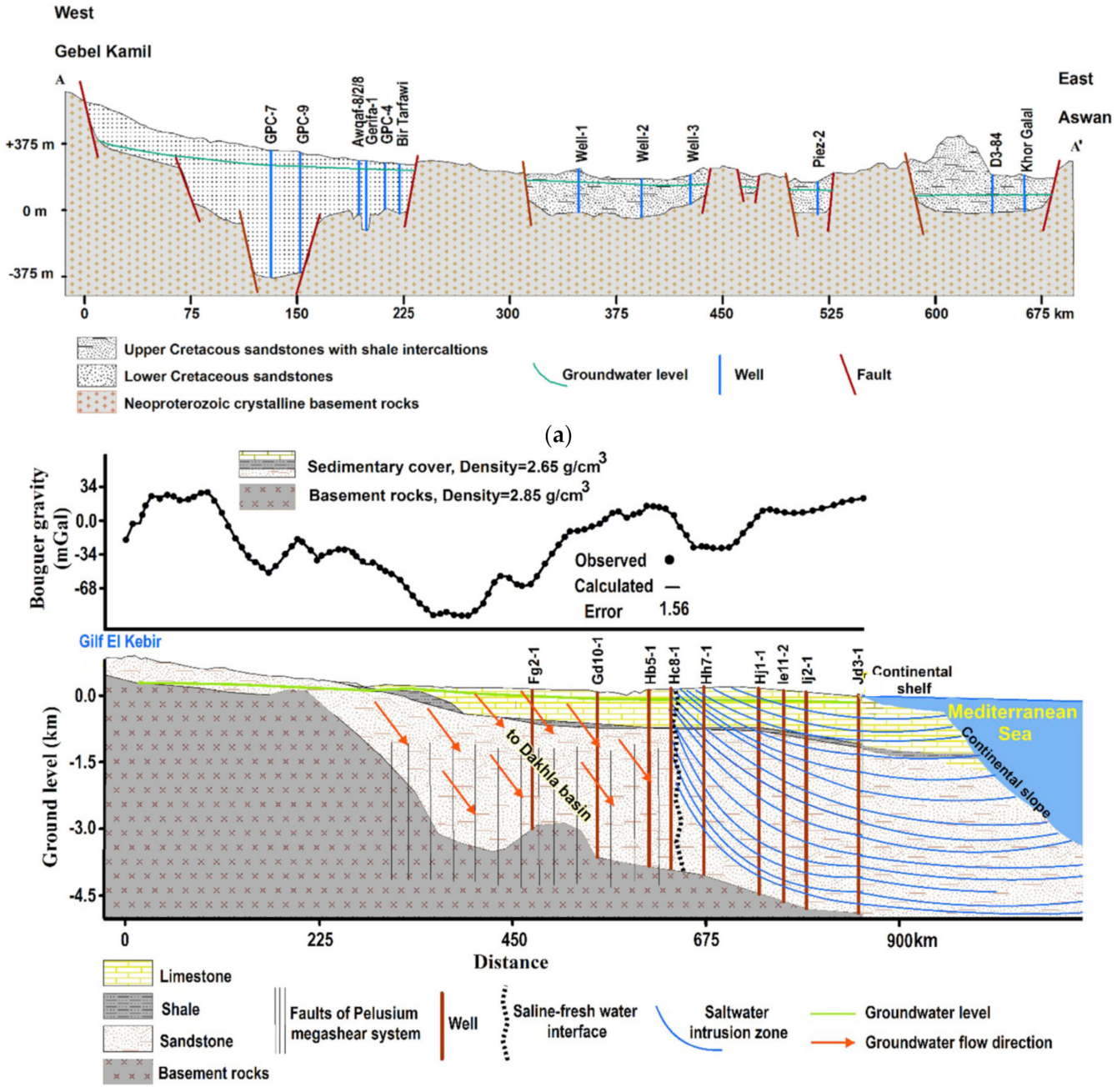

Figure 14. A geological west–east cross-section (**a**) along the Uweint–Aswan uplif [10,29]; and (**b**) A geological south–north cross-section along Gilf El Kebir-Mediterranean coast generated from modelling of gravity data and well data along the profile [29].

Based on the gravity interpretation results over the NSAS [10,29], the aquifer has a cross sectional area of 1000 km^2 along the Libyan-Egyptian border (Figure 14b) across the conduit of the shear zone, given a coefficient of average hydraulic conductivity of K = 5–7 $\times$ 10^{-5} m/s and a hydraulic gradient of h = 8 $\times$ 10^{-4}, the potential groundwater influx could amount to 1.26–1.77 km^3/y. In addition to employing gravity data in calculating the sedimentary cover across wide areas, it has been used with magnetic data for crustal thickness and heat flow studies (e.g., [66]), geometry of magma chamber (e.g., [67]), and groundwater studies (e.g., [37,68]).

6. Conclusions

The NSAS was recharged, according to our findings (recharge: plains: 2–7 mm/y; highlands: 10–27 mm/y) with a total average of ~8.13 mm/y (13.07 km^3/y) in the previous pluvial climatic period (>10,000 y) on a regional scale. This rate was enough to keep the aquifer full as close to the surface. During the filling-up condition, the groundwater flow direction was in a NE from the southwestern highlands of Ennedi, Erdi, and Tebesti, and in a NE from Uweinat highland towards the discharge areas, especially in the lower zones. The groundwater flow was redirected to a N direction in the shallow zones as the aquifer became full up to the surface 10 ky BP, and the north-trending Kufra paleorive was formed, that was probably active during the early Holocene and became dry 5–6 ky BP. The Uweinat area also showed a surface watershed down flowing in an ENE direction that might be active until 5–6 ky BP. The aquifer was in a naturally outflow process during the dry period (<10,000 y) along the depressions and the Nile River, in addition to artificial discharge after starting of the development projects in 1960 in Egypt and Libya, which were not balanced by natural flow and modest recharge from the south. As the water level in the aquifer continues to decrease, the E–W trending Uweinat–Aswan Basement uplift will gradually restrict groundwater flow from the N. Sudan Platform. The Pelusium megashear zone, which is northeast trending, is a favored conduit for groundwater flow from Kufra to the Dakhla Basin, and groundwater flow along that flow pathway refreshes the northern parts of the Dakhla Basin.

Author Contributions: Data curation, A.M. and E.A.; Formal analysis, A.M.; Funding acquisition, F.A.; Investigation, A.M. and E.A.; Methodology, A.M.; Resources, A.M. and A.A.; Software, A.M.; Visualization, F.A.; Writing—original draft, A.M.; Writing—review & editing, A.M., E.A. and A.A. All authors have read and agreed to the published version of the manuscript.

Funding: The APC was funded by the Abdullah Alrushaid Chair for Earth Science Remote Sensing Research.

Data Availability Statement: The data is available upon request from the first author.

Acknowledgments: The authors extend their appreciation to the Abdullah Alrushaid Chair for Earth Science Remote Sensing Research for funding.

Conflicts of Interest: The authors declare no conflict of interest.

References

1. Sarnthein, M.; Tetzlaff, G.; Koopmann, B.; Wolter, K.; Pflaumann, U. Glacial and interglacial wind regimes over the eastern subtropical Atlantic and North-West Africa. *Nature* **1981**, *293*, 193–196. [CrossRef]
2. Prell, W.L.; Kutzbach, J.E. Monsoon variability over the past 150,000 years. *J. Geophys. Res. Earth Surf.* **1987**, *92*, 8411–8425. [CrossRef]
3. Yan, Z.; Petit-Maire, N. The last 140 ka in the Afro-Asian arid/semi-arid transitional zone. *Palaeogeogr. Palaeoclim. Palaeoecol.* **1994**, *110*, 217–233. [CrossRef]
4. Sultan, M.; Sturchio, N.; Hassan, F.; Hamdan, M.A.R.; Mahmood, A.M.; El Alfy, Z.; Stein, T. Precipitation Source Inferred from Stable Isotopic Composition of Pleistocene Groundwater and Carbonate Deposits in the Western Desert of Egypt. *Quat. Res.* **1997**, *48*, 29–37. [CrossRef]
5. Sturchio, N.C.; Du, X.; Purtschert, R.; Lehmann, B.E.; Sultan, M.; Patterson, L.J.; Lu, Z.-T.; Müller, P.; Bigler, T.; Bailey, K.; et al. One million year old groundwater in the Sahara revealed by krypton-81 and chlorine-36. *Geophys. Res. Lett.* **2004**, *31*, L05503. [CrossRef]
6. Ball, J. Problems of the Libyan Desert. *Geogr. J.* **1927**, *70*, 21–38. [CrossRef]
7. Sandford, K.S. Sources of Water in the North-Western Sudan. *Geogr. J.* **1935**, *85*, 412–431. [CrossRef]
8. Brinkmann, P.J.; Heinl, M.; Hollander, R.; Reich, G. Retrospective simulation of groundwater flow and transport in the Nubian Aquifer system. *Berl. Geowiss. Abh. A* **1987**, *75*, 465–516.
9. Wright, E.P.; Benfield, A.C.; Edmunds, W.M.; Kitching, R. Hydrogeology of the Kufra and Sirte basins, eastern Libya. *Q. J. Eng. Geol. Hydrogeol.* **1982**, *15*, 83–103. [CrossRef]
10. Mohamed, A.; Sultan, M.; Ahmed, M.; Yan, E.; Ahmed, E. Aquifer recharge, depletion, and connectivity: Inferences from GRACE, land surface models, and geochemical and geophysical data. *Bull. Geol. Soc. Am.* **2017**, *129*, 534–546. [CrossRef]
11. Haynes, C.V.; Haas, H. Radiocarbon Evidence for Holocene Recharge of Groundwater, Western Desert, Egypt. *Radiocarbon* **1980**, *22*, 705–717. [CrossRef]

12. Hesse, K.-H.; Hissene, A.; Kheir, O.; Schnaecker, E.; Schneider, M.; Thorweihe, U. Hydrogeological investigations of the Nubian Aquifer System, Eastern Sahara. *Berl. Geowiss. Abh. A* **1987**, *75*, 397–464.
13. Thorweihe, U. The Nubian Aquifer System. In *The Geology of Egypt*; Said, R., Ed.; Balkema: Lisse, The Netherlands, 1990; pp. 601–614.
14. Sultan, M.; Sturchio, N.; Gheith, H.; Hady, Y.A.; Anbeawy, M. Chemical and Isotopic Constraints on the Origin of Wadi El-Tarfa Ground Water, Eastern Desert, Egypt. *Groundwater* **2000**, *38*, 743–751. [CrossRef]
15. Sultan, M.; Metwally, S.; Milewski, A.; Becker, D.; Ahmed, M.; Sauck, W.; Soliman, F.; Sturchio, N.; Yan, E.; Rashed, M.; et al. Modern recharge to fossil aquifers: Geochemical, geophysical, and modeling constraints. *J. Hydrol.* **2011**, *403*, 14–24. [CrossRef]
16. Tiwari, V.M.; Wahr, J.; Swenson, S. Dwindling groundwater resources in northern India, from satellite gravity observations. *Geophys. Res. Lett.* **2009**, *36*, L18401. [CrossRef]
17. Lenk, O. Satellite based estimates of terrestrial water storage variations in Turkey. *J. Geodyn.* **2013**, *67*, 106–110. [CrossRef]
18. Voss, K.A.; Famiglietti, J.S.; Lo, M.-H.; De Linage, C.; Rodell, M.; Swenson, S.C. Groundwater depletion in the Middle East from GRACE with implications for transboundary water management in the Tigris-Euphrates-Western Iran region. *Water Resour. Res.* **2013**, *49*, 904–914. [CrossRef]
19. Gonçalvès, J.; Petersen, J.; Deschamps, P.; Hamelin, B.; Baba-Sy, O. Quantifying the modern recharge of the "fossil" Sahara aquifers. *Geophys. Res. Lett.* **2013**, *40*, 2673–2678. [CrossRef]
20. Wouters, B.; Bonin, J.A.; Chambers, D.P.; Riva, R.E.M.; Sasgen, I.; Wahr, J. GRACE, time-varying gravity, Earth system dynamics and climate change. *Rep. Prog. Phys.* **2014**, *77*, 116801. [CrossRef]
21. Döll, P.; Schmied, H.M.; Schuh, C.; Portmann, F.T.; Eicker, A. Global-scale assessment of groundwater depletion and related groundwater abstractions: Combining hydrological modeling with information from well observations and GRACE satellites. *Water Resour. Res.* **2014**, *50*, 5698–5720. [CrossRef]
22. Huang, Z.; Pan, Y.; Gong, H.; Yeh, P.J.F.; Li, X.; Zhou, D.; Zhao, W. Subregional-scale groundwater depletion detected by GRACE for both shallow and deep aquifers in North China Plain. *Geophys. Res. Lett.* **2015**, *42*, 1791–1799. [CrossRef]
23. Huang, J.; Pavlic, G.; Rivera, A.; Palombi, D.; Smerdon, B. Mapping groundwater storage variations with GRACE: A case study in Alberta, Canada. *Hydrogeol. J.* **2016**, *24*, 1663–1680. [CrossRef]
24. Chinnasamy, P.; Agoramoorthy, G. Groundwater storage and depletion trends in Tamil Nadu State, India. *Water Resour. Manag.* **2015**, *29*, 2139–2152. [CrossRef]
25. Ahmed, M.; Sultan, M.; Yan, E.; Wahr, J. Assessing and Improving Land Surface Model Outputs Over Africa Using GRACE, Field, and Remote Sensing Data. *Surv. Geophys.* **2016**, *37*, 529–556. [CrossRef]
26. Jiang, Q.; Ferreira, V.G.; Chen, J. Monitoring groundwater changes in the Yangtze River basin using satellite and model data. *Arab. J. Geosci.* **2016**, *9*, 500. [CrossRef]
27. Lakshmi, V. Beyond GRACE: Using Satellite Data for Groundwater Investigations. *Groundwater* **2016**, *54*, 615–618. [CrossRef]
28. Long, D.; Chen, X.; Scanlon, B.R.; Wada, Y.; Hong, Y.; Singh, V.P.; Chen, Y.; Wang, C.; Han, Z.; Yang, W. Have GRACE satellites overestimated groundwater depletion in the Northwest India Aquifer? *Sci. Rep.* **2016**, *6*, 24398. [CrossRef]
29. Mohamed, A. Hydro-geophysical study of the groundwater storage variations over the Libyan area and its connection to the Dakhla basin in Egypt. *J. Afr. Earth Sci.* **2019**, *157*, 103508. [CrossRef]
30. Mohamed, A. Gravity based estimates of modern recharge of the Sudanese area. *J. Afr. Earth Sci.* **2020**, *163*, 103740. [CrossRef]
31. Mohamed, A. Gravity applications in estimating the mass variations in the Middle East: A case study from Iran. *Arab. J. Geosci.* **2020**, *13*, 364. [CrossRef]
32. Mohamed, A. Gravity applications to groundwater storage variations of the Nile Delta Aquifer. *J. Appl. Geophys.* **2020**, *182*, 104177. [CrossRef]
33. Mohamed, A.; Gonçalvès, J. Hydro-geophysical monitoring of the North Western Sahara Aquifer System's groundwater resources using gravity data. *J. Afr. Earth Sci.* **2021**, *178*, 104188. [CrossRef]
34. Mohamed, A.; Eldeen, E.R.; Abdelmalik, K. Gravity based assessment of spatio-temporal mass variations of the groundwater resources in the Eastern Desert, Egypt. *Arab. J. Geosci.* **2021**, *14*, 500. [CrossRef]
35. Taha, A.I.; Al Deep, M.; Mohamed, A. Investigation of groundwater occurrence using gravity and electrical resistivity methods: A case study from Wadi Sar, Hijaz Mountains, Saudi Arabia. *Arab. J. Geosci.* **2021**, *14*, 334. [CrossRef]
36. Mohamed, A.; Abdelrahman, K.; Abdelrady, A. Application of Time-Variable Gravity to Groundwater Storage Fluctuations in Saudi Arabia. *Front. Earth Sci.* **2022**, *10*, 873352. [CrossRef]
37. Mohamed, A.; Al Deep, M.; Othman, A.; Taha Al Alshehri, F.; Abdelrady, A. Integrated Geophysical Assessment of groundwater potential in southwestern Saudi Arabia. *Front. Earth Sci.* **2022**. *under review*.
38. Bellini, E.; Massa, D. A stratigraphic contribution to the Paleozoic of the southern basins of Libya. In *The Geology of Libya*; Salem, M.J., Brusrewi, M.T., Eds.; Elsevier: Amsterdam, The Netherlands, 1980; pp. 1–289.
39. Wycisk, P. Correlation of the major late Jurassic-Early Tertiary low- and high stand cycles of SW Egypt and NW Sudan. *Geol. Rsch.* **1994**, *83*, 759–772.
40. Klitzsch, E. Zur Stratigraphie Nubiens: Z. dt. *Geol. Ges.* **1989**, *140*, 151–160.
41. Said, R. Geomorphology. In *The Geology of Egypt*; Said, R., Ed.; Balkema: Rotterdam, The Netherlands, 1990; pp. 9–25.
42. Isotopic identification and mass balance of the Nubian Aquifer System in Egypt. In *Impact of Climatic Variations on East Saharian Groundwaters—Modelling of Large Scale Flow Regimes, Proceedings of a Workshop on Hydrology*; Series A; Thorweihe, U. (Ed.) Berliner Geowissenschaftliche Abhandlungen: Berlin, Germany, 1986; Volume 72, pp. 87–97.

43. Heinl, M.; Thorweihe, U. Groundwater Resources and Management in SW-Egypt. In *Geopotential and Ecology: Analysis of a Desert Region*; Catena Supplement; Meissner, B., Wycisk, P., Eds.; Margot Rohdenburg, Catena Verlag GmbH: Berlin, Germany, 1993; Volume 26, 199p.
44. Ebraheem, A.; Riad, S.; Wycisk, P.; Seif El-Nasr, A. Simulation of impact of present and future groundwater extraction from the non-replenished Nubian Sandstone Aquifer in southwest Egypt. *Environ. Earth Sci.* **2002**, *43*, 188–196. [CrossRef]
45. Gossel, W.; Ebraheem, A.M.; Wycisk, P. A very large scale GIS-based groundwater flow model for the Nubian sandstone aquifer in Eastern Sahara (Egypt, northern Sudan and eastern Libya). *Appl. Hydrogeol.* **2004**, *12*, 698–713. [CrossRef]
46. Lowe, J.J.; Walker, M.J.C. *Reconstructing Quaternary Environments*, 2nd ed.; Prentice Hall: Harlow, UK, 1997; p. 446.
47. Kehl, H.; Bornkamm, X. Landscape ecology and vegetation units of the Western Deserts of Egypt. *Catena* **1993**, *26*, 155–178.
48. Wendorf, F.; Schild, R. *Prehistory of the Eastern Sahara*; Academic Press: New York, NY, USA, 1980.
49. Pachur, H.J.; Braun, G. The palaeoclimate of the central Sahara, Libya, and the Libyan Desert. In *Palaeoecology of Africa*; Sarntheim, M., Siebold, E., Rognon, P., Eds.; Routledge; CRC Press: Boca Raton, FL, USA, 1980; Volume 12, pp. 351–363.
50. Kröpelin, S. Paleoclimatic evidence from early to mid-Holocene playas in the Gilf Kebir (Southwest Egypt). *Palaeoecol. Afr.* **1987**, *18*, 189–208.
51. Ritchie, J.C.; Eyles, C.H.; Haynes, C.V. Sediment and pollen evidence for an early to mid-Holocene humid period in the eastern Sahara. *Nature* **1985**, *314*, 352–355. [CrossRef]
52. Pachur, H.J.; Röper, H.P. The Libyan (Western) Desert and northern Sudan during the late Pleistocene and Holocene. *Berl. Geowiss. Abh. A* **1984**, *50*, 249–284.
53. Haynes, C.V., Jr.; Eyles, C.H.; Pavlish, L.A.; Ritchie, J.C.; Rybak, M. Holocene paleoecology of the eastern Sahara: Selima Oasis. *Quat. Sci. Rev.* **1989**, *8*, 109–136. [CrossRef]
54. Pachur, H.J.; Kröpelin, S.; Hoelzman, P.; Goschin, M.; Altmann, N. Late Quaternary fluvio-lacustrine environments of western Nubia. *Berl. Geowiss. Abh. A* **1990**, *120*, 203–260.
55. Kropelin, S. Lower Wadi Howar. *Berl. Geowiss. Abh. A* **1990**, *120*, 223–234, 256–259.
56. Thorweihe, U.; Heinl, M. *Groundwater Resources of the Nubian Aquifer System NE-Africa Synthesis: Modified Synthesis Submitted to Observatoire du Sahara et du Sahel*; OSS: Paris, France, 2002; p. 23.
57. Abouelmagd, A.; Sultan, M.; Sturchio, N.; Soliman, F.; Rashed, M.; Ahmed, M.; Kehew, A.E.; Milewski, A.; Chouinard, K. Paleoclimate record in the Nubian Sandstone Aquifer, Sinai Peninsula, Egypt. *Quat. Res.* **2014**, *81*, 158–167. [CrossRef]
58. Centre for the Environment and Development for the Arab Region and Europe (CEDARE). *Regional Strategy for the Utilization of the Nubian Sandstone Aquifer System-Hydrogeology*; CEDARE: Cairo, Egypt, 2001; Volume II.
59. Sonntag, C. A time dependent groundwater model for the Eastern Sahara. *Berl. Geowiss. Abh. A* **1986**, *72*, 124–134.
60. Sonntag, C.; Christmann, D. Groundwater evaporation from east Saharian depressions by measuring deuterium and oxygen-18 in soil moisture. *Berl. Geowiss. Abh. A* **1987**, *75*, 385–396.
61. Nour, S. Groundwater potential for irrigation in the East-Oweinat area, Western Desert, Egypt. *Environ. Geol.* **1996**, *27*, 143–154.
62. Patterson, L.J.; Sturchio, N.C.; Kennedy, B.M.; Van Soest, M.C.; Sultan, M.; Lu, Z.-T.; Lehmann, B.; Purtschert, R.; El Alfy, Z.; El Kaliouby, B.; et al. Cosmogenic, radiogenic, and stable isotopic constraints on groundwater residence time in the Nubian Aquifer, Western Desert of Egypt. *Geochem. Geophys. Geosyst.* **2005**, *6*, 1–19. [CrossRef]
63. Froehlich, K.; Aggarwal, P.K.; Garner, W.A. *An Integrated Approach in Evaluating Isotopic Data of the Nubian Sandstone Aquifer Syatem (NSAS) in Egypt (IAEA–CN–151/147): Advances in Isotope Hydrology and its Role in Sustainable Water Resources Management (IHS–2007), Proceedings of a Symposium in Vienna*; International Atomic Energy Agency (IAEA): Vienna, Austria, 2007; Volume 1, pp. 31–45.
64. Schneider, M.; Sonntag, C. Hydrogeology of the Gebel Uweinat-Aswan Uplift System, Eastern Sahara. In *Hydrogeology of Rocks of Low Permeability*; International Congress: Tucson, AZ, USA, 1985.
65. Sultan, M.; Ahmed, M.; Sturchio, N.; Eugene, Y.; Milewski, A.; Becker, R.; Wahr, J.; Becker, D.; Chouinard, K. Assessment of the vulnerabilities of the Nubian Sandstone Fossil Aquifer, North Africa. In *Climate Vulnerability. Understanding and Addressing Threats to Essential Resources*; Pielke, R.A., Ed.; Elsevier Inc.; Academic Press: Oxford, UK, 2013; Volume 5, pp. 311–333.
66. Mohamed, A.; Al Deep, M. Depth to the Bottom of the Magnetic Layer, Crustal Thickness, and Heat Flow in Africa: Inferences from Gravity an Magnetic Data. *J. Afr. Earth Sci.* **2021**, *179*, 104204. [CrossRef]
67. Mohamed, A.; Al Deep, M.; Abdelrahman, K.; Abdelrady, A. Geometry of the Magma Chamber and Curie Point Depth Beneath Hawaii Island: Inferences from Magnetic and Gravity data. *Front. Earth Sci.* **2022**, *10*, 847984. [CrossRef]
68. Othman, A.; Abdelrady, A.; Mohamed, A. Time-lapse gravity for estimating groundwater storage changes in Iraq. *Remote Sens.* **2022**. *under review*.